Current-pulse-induced magnetic switching in standard and nonstandard spin-valves: Theory and numerical analysis

P. Baláž,[1,*] M. Gmitra,[2] and J. Barnaś[1,3]
[1]*Department of Physics, Adam Mickiewicz University, Umultowska 85, 61-614 Poznań, Poland*
[2]*Institute of Physics, P. J. Šafárik University, Park Angelinum 9, 040 01 Košice, Slovak Republic*
[3]*Institute of Molecular Physics, Polish Academy of Sciences, Smoluchowskiego 17, 60-179 Poznań, Poland*
(Received 22 September 2008; revised manuscript received 16 February 2009; published 3 April 2009)

Magnetization switching due to a current pulse in symmetric and asymmetric spin-valves is studied theoretically within the macrospin model. The switching process and the corresponding switching parameters are shown to depend significantly on the pulse duration and also on the interplay between the torques due to spin transfer and external magnetic field. This interplay leads to peculiar features in the corresponding phase diagram. These features in standard spin-valves, where the spin-transfer torque stabilizes one of the magnetic configurations (either parallel or antiparallel) and destabilizes the opposite one, are different from those in nonstandard (asymmetric) spin-valves, where both collinear configurations are stable for one current orientation and unstable for the opposite one. Following this we propose a scheme of ultrafast current-induced switching in nonstandard spin-valves, based on a sequence of two current pulses.

DOI: 10.1103/PhysRevB.79.144301 PACS number(s): 67.30.hj, 75.60.Jk, 75.70.Cn

I. INTRODUCTION

The possibility of current-induced magnetic switching (CIMS) in multilayer structures has been introduced by Slonczewski[1] and Berger.[2] They pointed out that spin-polarized current passing through a multilayer consisting of two ferromagnetic layers separated by a nonmagnetic spacer can exert a torque on the local magnetic moments in ferromagnetic layers. In case of commonly used (standard) spin-valves, this torque can switch the system between parallel (P) and antiparallel (AP) alignments of the layers' magnetic moments. Indeed, the CIMS has been confirmed experimentally in many spin-valve structures.[3–6]

In order to meet the technological demands for applications, designing of bistable magnetic spin-valve devices that could be fast switched by electric current only is highly desired. Accordingly, several subtle switching schemes aimed at speeding up the switching process and lowering the energy costs have been developed for various magnetic multilayer structures. It has been shown that proper optimization of the current-pulse parameters (amplitude, duration, frequency, etc.) can finally result in ultrafast single-step switching.[7,8]

Current-induced dynamics in spin-valves is governed by spin-transfer torque (STT), particularly by its magnitude and dependence on the angle between magnetization vectors of the reference and sensing magnetic layers. Such an angular variation depends mainly on the type of electron transport through the spin-valve. Recently, STT in the diffusive transport regime draws more attention. It has been demonstrated[9] that spin diffusion in various types of polarizing layer can strongly influence the current-induced behavior of spin-valves. To calculate STT in the diffusive transport limit, one can consider the model[10] that extends the Valet-Fert description[11] to arbitrary magnetic configuration and allows us to study STT as a function of layers' thicknesses, type of materials, spin asymmetries, etc, which can be directly compared to experimental observations.[12] In the case of diffusive transport, spin-diffusion length has to be much longer than the mean-free path. However, it has been shown[13] that diffusive approach is valid also for spin-diffusion lengths of the order of mean-free paths. Moreover, the approach describes relatively well experimental results even for layer thicknesses comparable to the corresponding mean-free paths.

One of the most pronounced manifestation of the importance of spin-diffusion length has been shown for asymmetric spin-valves,[10] where the nonstandard (wavylike) angular dependence of STT leads to the current-induced precessional regimes in zero magnetic field.[14–16] This prediction has been later confirmed experimentally.[17,18] The wavylike STT vanishes not only in the collinear configurations—P and AP ones—but also in a certain noncollinear configuration. Depending on the current direction, the collinear configurations are either both stable or both unstable. The first case is of importance for the current-induced zero-field microwave excitations, while the latter one would be desired for further stabilization of the collinear magnetic configurations in memory devices against thermal or current fluctuation. Since the problem of switching in nonstandard spin-valves has not been addressed yet, here we present a comprehensive study of the CIMS in such systems due to a current pulse of finite duration. In the following, the spin-valves with wavylike STT will be refereed to interchangeably as nonstandard or asymmetric one, whereas the spin-valves with STT vanishing only in collinear configurations will be referred to as standard or symmetric one.

In this paper, we investigate current-pulse-induced magnetization dynamics in three-layer spin-valve $X/\mathrm{Cu}(10)/\mathrm{Py}(8)$ sandwiched between semi-infinite Cu leads. The numbers in brackets correspond to the layers' thicknesses in nanometers. Py(8) stands for the Permalloy sensing layer, which magnetization direction can freely rotate upon applied magnetic field and/or spin-polarized current, whereas X denotes the reference layer, which magnetization is considered to be fixed and not influenced by external magnetic fields and electric current. Assuming these conditions, we have considered two different types of the reference layer:

X=Py(20) and X=Co(8). Taking into account the above introduced notation, the former spin-valves, Py/Cu/Py, will be referred to as standard or symmetric, whereas the latter spin-valves, Co/Cu/Py, we will be referred to as nonstandard or asymmetric one.

The main motivation of this paper is to provide a systematic study of the CIMS based on the macrospin simulations. We consider a rectangular current pulse characterized by the current amplitude and pulse duration. We have found that a proper choice of the pulse parameters leads to fast switching with relatively low energy costs. In the case of nonstandard spin-valves, the double-pulse scheme, which allows reliable switching between the collinear magnetic configurations and significant shortening of the overall switching time, is proposed.

The paper is organized as follows. In Sec. II we describe the macrospin model. Numerical analysis for both standard and nonstandard (asymmetric) spin-valves is described in Sec. III, where also a double-pulse switching scheme for an asymmetric spin-valve is described. Section IV includes summary and final conclusions.

II. MACROSPIN MODEL

Time-resolved imaging of CIMS showed that inhomogeneous spatiotemporal magnetization evolution takes place during the reversal.[19] Thus, more sophisticated models, involving detailed micromagnetic description, have to be adopted for a better qualitative description.[20] However, the macrospin model—particularly for spin-valves in nanosize range—provides a sufficient quantitative description of the current-induced dynamics, which is in agreement with many experiments on standard spin-valves.[6] A relatively good qualitative agreement has been reached also for nonstandard (asymmetric) spin-valves, where some predictions based on the macrospin model[14–16] have been confirmed experimentally.[17,18]

The time evolution of the unit vector $\hat{\boldsymbol{s}}=(s_x,s_y,s_z)$ along the net spin moment of the sensing layer is described by the generalized Landau-Lifshitz-Gilbert (LLG) equation

$$\frac{d\hat{\boldsymbol{s}}}{dt}=-|\gamma_g|\mu_0\hat{\boldsymbol{s}}\times\boldsymbol{H}_{\mathrm{eff}}-\alpha\hat{\boldsymbol{s}}\times\frac{d\hat{\boldsymbol{s}}}{dt}+\frac{|\gamma_g|}{M_s d}\boldsymbol{\tau}, \tag{1}$$

where γ_g is the gyromagnetic ratio, μ_0 is the magnetic vacuum permeability, M_s is the saturation magnetization, and d is the sensing layer thickness. The Gilbert damping parameter α is assumed to be constant, α=0.01. The effective field $\boldsymbol{H}_{\mathrm{eff}}$ includes contributions from the external magnetic field (H_{ext}), uniaxial magnetic anisotropy (H_{ani}), demagnetization field ($\boldsymbol{H}_{\mathrm{dem}}$), and the thermal field ($\boldsymbol{H}_{\mathrm{th}}$); $\boldsymbol{H}_{\mathrm{eff}}=-H_{\mathrm{ext}}\hat{\boldsymbol{e}}_z-H_{\mathrm{ani}}(\hat{\boldsymbol{s}}\cdot\hat{\boldsymbol{e}}_z)\hat{\boldsymbol{e}}_z+\boldsymbol{H}_{\mathrm{dem}}+\boldsymbol{H}_{\mathrm{th}}$, where $\hat{\boldsymbol{e}}_z$ is the unit vector along the axis z which is parallel to the in-plane magnetic easy axis. By definition, the external field is positive when it is pointing along the negative z axis. The demagnetization field corresponds to the sensing layer of an elliptical shape with the major and minor axes of 130 and 60 nm, respectively, and thickness of 8 nm. The magnetic easy axis is assumed to be along the longer axis of the ellipse, and H_{ani}=100.5 Oe.

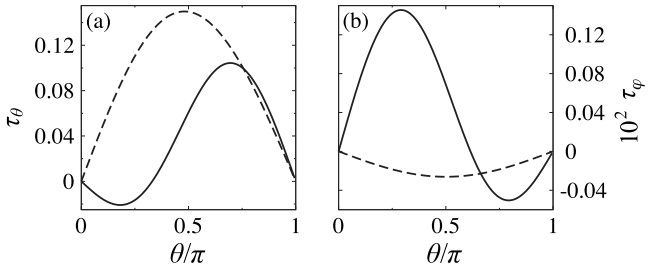

FIG. 1. Angular dependence of the spin-transfer torque components in units of $\hbar I/|e|$ acting on Py(8) in the Cu/X/Cu(10)/Py(8)/Cu spin-valves for the standard case with X=Py(20) (dashed lines) and nonstandard case (wavylike torque) with X=Co(8) (solid lines). (a) In-plane component τ_θ and (b) out-of-plane component τ_φ. The other parameters are as in Refs. 10 and 16.

The thermal field $\boldsymbol{H}_{\mathrm{th}}$ contributing to $\boldsymbol{H}_{\mathrm{eff}}$ is a stochastic field of statistical properties $\langle H_{\mathrm{th},i}(t)\rangle=0$ and $\langle H_{\mathrm{th},i}(t)H_{\mathrm{th},j}(t')\rangle=2\mathcal{D}\delta_{ij}\delta(t-t')$, where $i,j\in\{x,y,z\}$. The strength of the thermal fluctuations is given by the parameter $\mathcal{D}=2k_BT/[M_s(1+\alpha^2)]$ derived according to the fluctuation-dissipation relation,[21,22] with T being the temperature.

As concerns the STT, we consider both the in-plane and out-of-plane components $\boldsymbol{\tau}=\boldsymbol{\tau}_\theta+\boldsymbol{\tau}_\varphi$, where $\boldsymbol{\tau}_\theta=aI\hat{\boldsymbol{s}}\times(\hat{\boldsymbol{s}}\times\hat{\boldsymbol{S}})$ and $\boldsymbol{\tau}_\varphi=bI\hat{\boldsymbol{s}}\times\hat{\boldsymbol{S}}$. The vector $\hat{\boldsymbol{S}}$ points along the net spin of the reference layer X, $\hat{\boldsymbol{S}}=\hat{\boldsymbol{e}}_z$, and is assumed to be constant in time (current does not excite magnetic moment of the reference layer). Current density I is defined as positive when current flows from the reference layer toward the sensing one. Finally, the angular dependence of the parameters a and b has been calculated in the diffusive transport limit.[10] The resulting in-plane and out-of-plane torques for the spin-valves X/Cu(10)/Py(8) with X=Py(20) and Co(8) are shown in Fig. 1 as a function of the angle θ (azimuthal angle) between the magnetic moments of the reference and sensing layers ($\hat{\boldsymbol{s}}\cdot\hat{\boldsymbol{S}}=\cos\theta$).

III. NUMERICAL RESULTS

Here we study switching in the X/Cu(10)/Py(8) valves from the P to AP state due to a current pulse. Numerical solution of the LLG equation has been performed using the Heun scheme[23] with an autoadaptive time step. For the initial configuration we assume a biased state with $\theta(t=0)=1°$ and $\varphi(t=0)=\pi/2$, where φ is the polar angle describing orientation of the vector $\hat{\boldsymbol{s}}$ from the x axis parallel to the current flow. The current pulse $i(t)$ of constant current density I and duration t_p is applied at $t=0$, $i(t)=I[\Theta(t)-\Theta(t-t_p)]$, where $\Theta(x)=1$ for $x>0$ and $\Theta(x)=0$ for $x\leq 0$. A successful switching event with the corresponding switching time t_s is counted when $\bar{s}_z(t_s)<-0.99$, where $\bar{s}_z(t)$ is the exponentially weighted moving average,[24] $\bar{s}_z(t)=\eta s_z(t)+(1-\eta)\bar{s}_z(t-\Delta t)$, Δt is the integration step, and the weighting parameter η=0.1. The moving average $\bar{s}_z$ is calculated for time $t>t'$ when $s_z(t')$ reaches the value of −0.9; otherwise, $\bar{s}_z(t)=s_z(t)$. From the experimental point of view it is more convenient to reformulate the switching condition in terms of the magne-

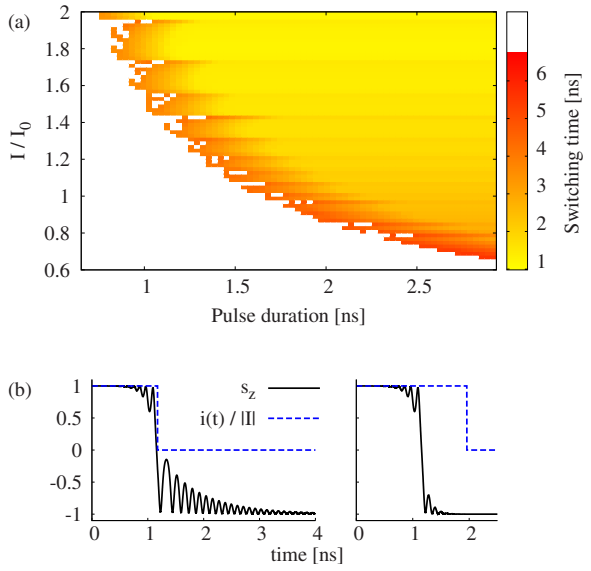

FIG. 2. (Color online) Current-pulse-driven switching in the Py(20)/Cu(10)/Py(8) spin-valve in the absence of magnetic field. (a) Switching time as a function of the pulse duration t_p and reduced current density I/I_0, where $I_0=10^8$ A cm^{-2}. (b) Temporal evolution of the s_z spin component under rectangular current pulse (dashed lines) of amplitude $I/I_0=1.4$ and duration $t_p=1.2$ ns (retarded switching, left) and $t_p=2$ ns (*fast switching*, right), corresponding to the points marked in the switching diagram (a).

toresistance. We note that this holds only for the standard spin-valves, in which the magnetoresistance is a monotonic function of the θ angle.[25,26] In asymmetric spin-valves the magnetoresistance can be a nonmonotonic function of θ,[26,27] and therefore direct calculation of the magnetoresistance is then needed.

A. Dynamics in a Py/Cu/Py spin-valve

Let us study first the standard spin-valve, X=Py(20). The in-plane and out-of-plane components of the STT acting on the Py(8) sensing layer show sinelike angular dependences (see dashed lines in Fig. 1). Switching time as a function of the pulse duration t_p and reduced current density I/I_0 ($I_0=10^8$ A cm^{-2}) is shown in Fig. 2(a). Here, we consider zero-temperature limit and the external magnetic field is set to zero. Two different regions in the switching diagram can be distinguished. First, the white nonswitching region is observed for short current pulses and low current densities. In this region, the energy gain due to STT does not overcome the Gilbert damping and system stays in the initial local magnetic energy minimum. The second region corresponds to successful switching to the AP state. The switching time t_s is shown in the gray scale. t_s decreases nonmonotonously with increasing current density. The brightest area corresponds to the ultrafast switching, in which the spin reaches the AP configuration before the current pulse ends ($t_s<t_p$). In such a case the switching is realized in a single ultrafast step after a half precession around the x axis [see Fig. 2(b), right].

The boundary between nonswitching and ultrafast switching regions develops into a ripple structure. In this region, the energy gain due to spin transfer leads to a *retarded switching*, where the switching time $t_s>t_p$ [see Fig. 2(b), left]. The switching for $t>t_p$ is accompanied with a ringing, where the spin relaxes to the AP state due to energy dissipation via the Gilbert damping only. Such dissipation, however, is rather slow and therefore the retarded switching is much slower than the ultrafast single-step switching.

To speed up switching from P to AP state one may consider a negative external magnetic field. On the other hand, a positive magnetic field exceeding the anisotropy field leads to commonly observed steady-state out-of-plane precessional (OPP) modes,[4–6] which are the result of the energy balance between Gilbert damping and the energy gain due to spin transfer.

Our analysis shows that for positive external magnetic field, the continuous switching region in the diagram shown in Fig. 2(a) splits into a noncompact current-dependent stripe structure. In Fig. 3(a) we show the switching diagram for $H_{\text{ext}}=200$ Oe. The switching regions alternate with the stripes where the spin transfer induces the OPP regime. Since the current pulse is finite, the final state depends on the actual spin state at $t=t_p$, which falls into the basin of attraction either of P or AP state. This is shown in Fig. 3(b), where two switching events under the current pulses of the same amplitude ($I=2.75I_0$) and different pulse durations are driven via the OPP regime. We note that in the switching regions the spin dynamics is similar to the zero-field switching discussed above.

To elucidate the stripe structure, we plotted in Fig. 3(c) map of the final spin states as a function of the initial spin position $\hat{s}_0=\hat{s}(t=0)$, assuming constant current amplitude and pulse duration $t_p\to\infty$. The gray (black) regions correspond to the initial spin position, which results in the final OPP (AP) regime. Comparing the maps calculated for two different current densities ($I=2.75I_0$ and $I=3.00I_0$), one concludes that the dynamical phase portrait depends rather strongly on the current density. In other words, current-driven dynamics from the same initial state can develop to different final states. Further increase in external magnetic field leads to shrinking of the P$\to$AP switching stripes. For fields much larger than the coercive field the switching stripes disappear so the OPP regime remains only. We note that the initial spin position (close to the P configuration) assumed in this paper [except Fig. 3(c)] is denoted in Fig. 3(c) by the circles.

The sharp stripe structure is a result of deterministic dynamics and fixed initial condition. When a distribution of initial configurations is taken into account, some smearing of the border between the stripes is observed (not shown). The boundaries are also smeared when nonzero temperature is considered. In Fig. 3(d) we show the switching probabilities as a function of the current pulse density calculated for pulse duration $t_p=3$ ns at $T=4.2$ K and $T=77$ K and for fixed initial configuration. The statistics has been calculated from 10^4 events for each value of the current density. The switching probability follows the stripe structure in the zero-temperature limit and decreases with decreasing current amplitude. For $T=77$ K, the probability is lowered by the factor of about 3 and the peaks broaden. From this follows that smearing of the boundaries between switching and precessional regions increases with increasing temperature. In ad-

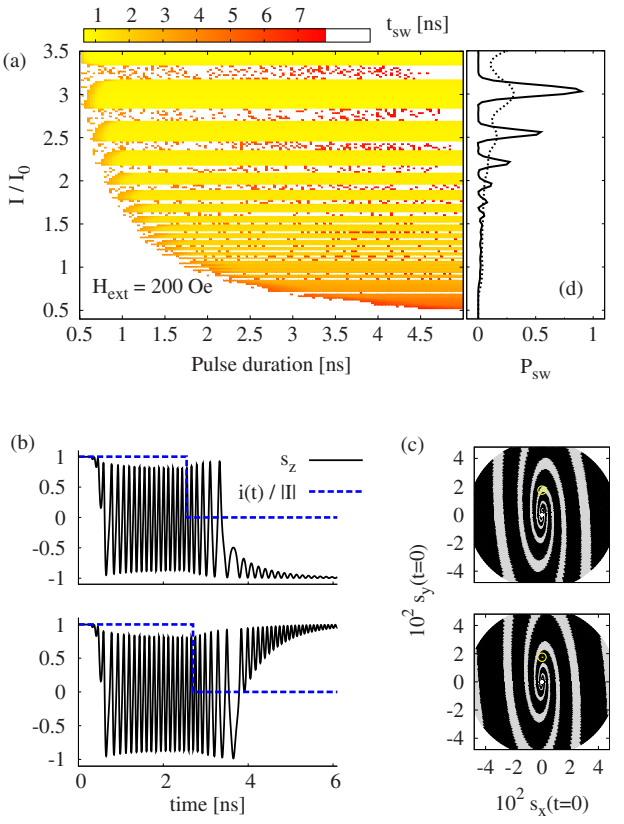

FIG. 3. (Color online) Effect of the external magnetic field $H_{\text{ext}}=200$ Oe on the current-pulse-driven dynamics in the Py(20)/Cu(10)/Py(8) spin-valve. (a) Switching time as a function of reduced current density I/I_0 ($I_0=10^8$ A cm^{-2}) and pulse duration t_p. (b) Temporal evolution of the s_z spin component under current pulses (dashed lines) marked in the switching diagram (a), corresponding to the amplitude $I=2.75I_0$ and durations $t_p=2.56$ ns (upper part) and $t_p=2.7$ ns (lower part). (c) The maps of the final states as a function of initial spin bias for current pulse of $I=2.75I_0$ (upper part) and $I=3.0I_0$ (lower part) and for $t_p\rightarrow\infty$. The spin dynamics initialized from the points inside the gray (black) areas leads finally to OPP regime (AP state). Circles denote the initial spin bias used in the simulations. (d) Thermally assisted switching probability P_{sw} from P to AP state driven by a 3 ns rectangular current pulse and calculated as a function of current density at $T=4.2$ K (solid line) and $T=77$ K (dotted line).

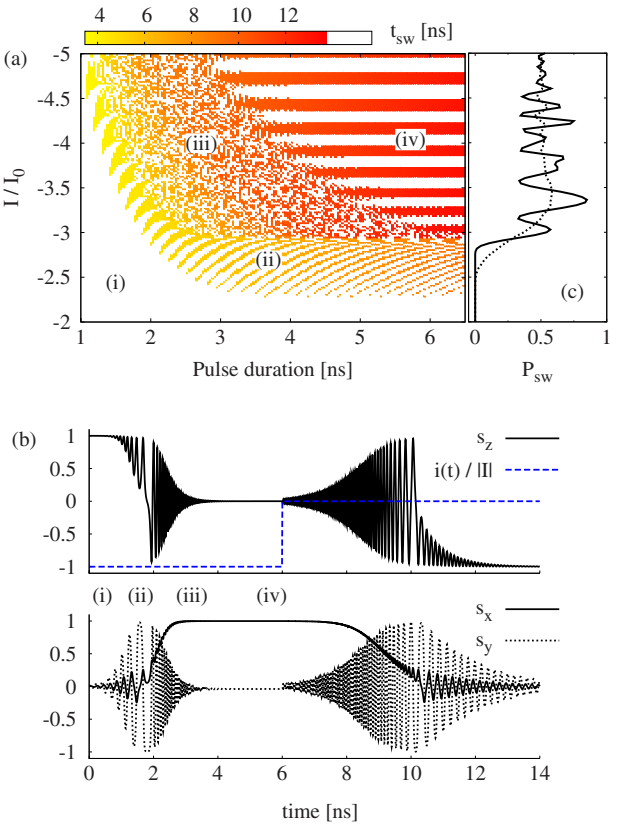

FIG. 4. (Color online) Current-pulse-induced switching in the asymmetric Co(8)/Cu(10)/Py(8) spin-valve at zero magnetic field. (a) Switching time as a function of the pulse duration t_p and reduced current density I/I_0, where $I_0=10^8$ A cm^{-2}. (b) Temporal evolution of $\hat{s}$ under the 6 ns current pulse of the amplitude $I=-3.45I_0$. (c) Thermally assisted switching probability P_{sw} from P to AP driven by 6 ns rectangular current pulse and calculated as a function of current density at $T=4.2$ K (solid line) and $T=77$ K (dotted line).

dition, positions of the peaks are shifted, which reflects the fact that thermal fluctuations act on the spin like an additional torque and nonlinearly influence the spin dynamics.

B. Dynamics in a Co/Cu/Py spin-valve

The Co(8)/Cu(10)/Py(8) spin-valve exhibits nonstandard STT acting on the Py(8) layer. Due to the *wavy*like dependence of the STT, shown by the solid lines in Fig. 1, positive current stabilizes both the P and AP configurations. A negative current, in turn, destabilizes both the collinear configurations. This characteristic property of the wavy torque raises the question, whether it is possible to switch an asymmetric spin-valve between P and AP states without the need of an external magnetic field.

In Fig. 4(a) we show the switching diagram from P to AP state under a rectangular current pulse. Here one may distinguish four characteristic switching regions. The first region, denoted by (i), corresponds to low current amplitudes and/or short pulses, where switching does not take place. The noncompact region (ii) of riblike structure borders the nonswitching region and comprises relatively short pulses leading to the fast switching processes. In region (iii) the P/AP bistability of the final states is observed. Finally, in region (iv) the final state of the dynamics depends on the applied current density, resulting in the bandlike structure. The structure contains regions with final P state, which regularly alternate with the regions of final AP state.

In order to explain the complex diagram structure, let us study current-pulse-induced dynamics due to the 6 ns pulse of amplitude $I=-3.45I_0$ at zero temperature. The temporal dependence of the spin components is shown in Fig. 4(b). When the constant current pulse is applied (in zero external magnetic field), it induces initially small-angle in-plane precessions (IPPs) of the sensing layer around the z axis. The precessional angle rapidly increases and spin dynamics turns to the OPP regime, where spin precesses mainly around the

demagnetization field. The out-of-plane component of the STT, $\boldsymbol{\tau}_{\varphi}$, assists in the transition to the OPP-like regime.[14] Numerical analysis reveals that the transition depends on the current amplitude, and spin can precess with positive or negative s_x component. Considering constant initial spin direction, OPP direction depends mainly on the current density. This appears because the spin phase portrait, and hence the spin trajectory, is modified due to the current density. Such a situation is similar to that discussed in Fig. 3(c) for the Py/Cu/Py spin-valve. Due to the sustained energy pumping to the system via the spin transfer, the OPP angle decreases and the spin is finally driven into one of the possible static states (SS) close to the $\hat{\boldsymbol{e}}_x$ (SS_+), or $-\hat{\boldsymbol{e}}_x$ (SS_-), depending on the sign of the s_x component in the OPP regime. The $SS_{\pm}$ states are the static fixed points that result from the interplay between the STT and effective magnetic field (mainly its demagnetization part). The $SS_{\pm}$ points are close to the maximum magnetic energy. Therefore, if current is turned off, the spin position becomes unstable; spin is driven due to Gilbert damping through the OPP regime with decreasing precessional frequency to the IPP regime. In the IPP regime, spin precesses around $+\hat{\boldsymbol{e}}_z$ ($-\hat{\boldsymbol{e}}_z$) direction and is finally damped to the P (AP) state. We have observed that position of the spin in SS_- (SS_+) results in the final P (AP) state [see Fig. 4(b)]. Thus the alternation between P and AP states in region (iv) in the diagram shown in Fig. 4(a) is predominantly controlled by the current since the position of the static state depends on the current density.

To elucidate other regions in the diagram [Fig. 4(a)], we have to consider shorter pulses. According to the diagram, to have a successful switching event, the pulse has to exceed a critical current density and duration. In the static limit ($t_p \rightarrow \infty$) the critical density is about $I=-1.0I_0$. For a finite pulse duration, higher densities are necessary to drive the spin during the time t_p away from the P state. When the pulse is shorter than a critical one, the relaxation back to the P state takes place [region (i)]. To escape the basin of attraction, the time t_p has to exceed an escape time that depends on the actual magnetic energy and the current density. For the higher current densities, the spin is driven faster away and a shorter escape time is needed. If the pulse ends just before the onset of the OPP regime, the spin is then placed within the basin of attraction of the AP state. The relaxation via the Gilbert dissipation drives the system to the AP state [region (ii)]. If the spin is driven further away from the P state, the IPP regime switches fast to the OPP one. In such a case the final state strongly depends on the precession phase at $t=t_p$, i.e., when the current is turned off. This gives rise to the P/AP bistability in region (iii). The bistable regime appears up to the pulse duration that is not longer than the time necessary for spin stabilization in the $SS_{\pm}$ state. Note, that this analysis is valid only for current amplitudes $I \gtrsim 3I_0$. In case of smaller amplitudes, only the steady-state large-angle IPP regime has been observed, and apart from region (i) only region (ii) is present. The periodic riblike structure in region (ii) arises from the dependence of the final state on the precession phase at time $t=t_p$.

When temperature is nonzero, the final state is affected by the thermal noise that modifies the overall spin switching trajectory. In Fig. 4(c) we show switching probability as a function of the current density for $t_p=6$ ns and $T=4.2$ K (solid line) and $T=77$ K (dotted line). The switching probability oscillates following the zero-temperature stripe structure, similarly as for the spin-valve Py(20)/Cu(10)/Py(8) [see Fig. 3(b)]. However, the probability P_{sw} oscillates now around the value of $P_{\mathrm{sw}}=0.5$ and for increased current densities approaches this value for any temperature. We have found that for higher current densities the spin is driven via the OPP-like transient regime much closer to the SS state. This regime is sensitive to the thermal fluctuations mainly due to the component of the thermal field transverse to the spin trajectory. When the spin remains in the transient regime for a longer time, the impact of the thermal fluctuations is larger and leads to equilibration of the probabilities for switching to the P and AP states ($P_{\mathrm{sw}} \rightarrow 0.5$).

C. Switching in nonstandard spin-valves

The fastest switching process in the asymmetric spin-valves appears in region (ii) [see Fig. 4(a)]. This region, however, is noncompact and therefore to obtain a successful switching one has to set the current pulse parameters very precisely. In region (iii) the bistability of the final state makes the switching out of control. Thus, the most convenient for switching seems to be region (iv). For a proper choice of parameters (pulse duration and current amplitude, including also the thermal effects), corresponding to the maximum of P_{sw} [see Fig. 4(c)], it is possible to obtain controllable switching. However, complex spin dynamics, especially the ringing which appears after the end of current pulse, significantly lengthen the switching time. In practice, the longer the switching time, the more sensitive is the spin evolution to the external disturbances and temperature. Therefore, it is highly desired from the applications point of view to shorten the switching time as much as possible. Accordingly, we propose here a double-pulse switching scheme. The scheme includes two rectangular current pulses of certain amplitudes and durations. The first pulse of negative current, referred to as *destabilizing pulse*, drives the spin out of its initial position. We note that both the collinear configurations are now unstable. The second pulse of positive current, called *stabilizing pulse*, controls the dynamics and drives the spin into the final state. Moreover, the stabilizing pulse shortens the switching time (suppressing the ringing) via additional energy dissipation from the system.

In Fig. 5(a) we show time evolution of the s_z component due to single current pulse and double current pulse. Here we consider infinitely long stabilizing pulse that in principle has no effect on the spin dynamics for $t \gtrsim 6.5$ ns. Due to the first current pulse of density $I=-4.0I_0$, the STT drives the spin to the SS state. When the first pulse is not followed by the second (stabilizing) one, the spin returns back via the OPP and IPP regimes to the initial state. In the case of double pulse, however, the stabilizing pulse of $I=2.0I_0$ drives the spin to the AP state. More systematical study reveals that including the stabilizing current pulse of $I=2I_0$ leads to considerable modification of the switching diagram (not shown). More specifically, region (ii) becomes wider and switching times under these current pulses fall down from 4 to 1 ns.

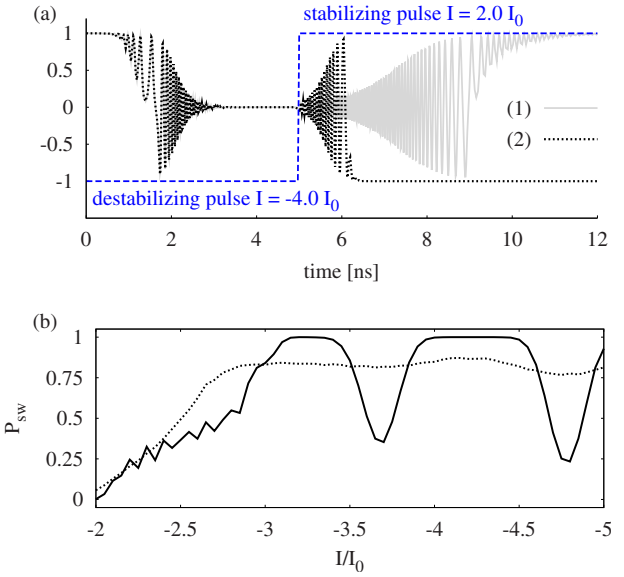

FIG. 5. (Color online) Demonstration of *double-pulse switching scheme* making use of second (stabilizing) pulse. (a) Evolution of s_z spin component. Line (1) corresponds to a single $t_p=5$ ns (destabilizing) current pulse of amplitude $I=-4.0I_0$ in zero magnetic field and zero temperature. Line (2) shows the evolution of s_z in the case when the first pulse is followed by a second (stabilizing) pulse of opposite direction and $I=2.0I_0$ (the double current pulse is shown by the dashed line). (b) Thermally assisted switching probability P_{sw} from the P to AP states, driven by a 5 ns (destabilizing) current pulse (negative), followed by a stabilization current pulse of $I=2.0I_0$ and $t_p\to\infty$, and calculated as a function of the reduced current density I/I_0 of the destabilizing pulse, $I_0=10^8$ A cm^{-2}, for $T=4.2$ K (solid line) and $T=77$ K (dotted line).

Bistability in region (iii) becomes reduced, but still not completely removed. Finally, in region (iv) the bands related to switching become enlarged, e.g., at $T=0$ K, in the range of amplitudes from $I\simeq-3.5I_0$ to $-4.5I_0$, one obtains controllable switching for pulses $t_p\gtrsim4$ ns. Further manipulation of the stabilizing pulse amplitude, indeed, enhances overall controllability of the switching.

In addition to the enhanced controllability due to the stabilizing pulse, we have observed enhancement of the switching probability at finite temperatures. In Fig. 5(b) we show the switching probability as a function of the current density of 5 ns destabilizing pulse that is followed by a stabilization current pulse of $I=2.0I_0$ and $t_p\to\infty$. For $T=4.2$ K and $I<-3I_0$, the probability P_{sw} oscillates with increasing current magnitude, similarly as in the case of a single pulse [see Fig. 4(c)]. The regions of successful switching are then broadened and the corresponding amplitude is close to unity. In the case of $T=77$ K, the switching probability in this region is roughly constant and approaches $P_{\mathrm{sw}}\simeq0.8$.

IV. SUMMARY AND CONCLUSIONS

We have studied dynamics of the current-pulse-induced magnetization switching in both standard and nonstandard spin-valves. The calculated switching diagrams reveal the pulse parameters that are suitable for ultrafast spin switching. We showed that the schemes of optimal switching strongly depend on the type of pillar structure and are different for standard and nonstandard spin-valves. The wavylike torque in nonstandard spin-valves introduces stable points in the phase portrait for negative currents. These stable points are responsible for the P/AP bistability in the pulse switching diagram, which hinders obtaining successful switching. Therefore, we proposed a switching scheme by making use of two current pulses, which can efficiently overcome the bistable behavior. Additionally, the application of second positive current pulse speeds up the spin dynamics and fastens the switching process for several times. We have also shown that the proposed scheme leads to enhanced switching probability even at high temperatures.

ACKNOWLEDGMENTS

The work was supported by the EU through the Marie Curie Training network SPINSWITCH (Contract No. MRTN-CT-2006-035327). M.G. acknowledges support within research projects MVTS under Contract No. POL/SR/UPJS07 and VEGA under Contract No. 1/0128/08. J.B. acknowledges support from the Polish Ministry of Science and Higher Education as a research project in years 2006–2009 and National Scientific network ARTMAG. P.B. thanks E. Jaromirska and L. López-Díaz for helpful discussions.

*balaz@amu.edu.pl

[1] J. C. Slonczewski, J. Magn. Magn. Mater. **159**, L1 (1996).
[2] L. Berger, Phys. Rev. B **54**, 9353 (1996).
[3] M. Tsoi, A. G. M. Jansen, J. Bass, W.-C. Chiang, M. Seck, V. Tsoi, and P. Wyder, Phys. Rev. Lett. **80**, 4281 (1998).
[4] E. B. Myers, D. C. Ralph, J. A. Katine, R. N. Louie, and R. A. Buhrman, Science **285**, 867 (1999).
[5] J. A. Katine, F. J. Albert, R. A. Buhrman, E. B. Myers, and D. C. Ralph, Phys. Rev. Lett. **84**, 3149 (2000).
[6] S. I. Kiselev, J. C. Sankey, I. N. Krivorotov, N. C. Emley, R. J. Schoelkopf, R. A. Buhrman, and D. C. Ralph, Nature (London) **425**, 380 (2003).
[7] S. Serrano-Guisan, K. Rott, G. Reiss, J. Langer, B. Ocker, and H. W. Schumacher, Phys. Rev. Lett. **101**, 087201 (2008).
[8] S. Garzon, L. Ye, R. A. Webb, T. M. Crawford, M. Covington, and S. Kaka, Phys. Rev. B **78**, 180401(R) (2008).
[9] S. Urazhdin and S. Button, Phys. Rev. B **78**, 172403 (2008).
[10] J. Barnas, A. Fert, M. Gmitra, I. Weymann, and V. K. Dugaev, Phys. Rev. B **72**, 024426 (2005).
[11] T. Valet and A. Fert, Phys. Rev. B **48**, 7099 (1993).
[12] S. Urazhdin, N. O. Birge, W. P. Pratt, and J. Bass, Phys. Rev. Lett. **91**, 146803 (2003).
[13] D. R. Penn and M. D. Stiles, Phys. Rev. B **72**, 212410 (2005).
[14] M. Gmitra and J. Barnaś, Phys. Rev. Lett. **96**, 207205 (2006).

[15] M. Gmitra and J. Barnaś, Appl. Phys. Lett. **89**, 223121 (2006).
[16] M. Gmitra and J. Barnaś, Phys. Rev. Lett. **99**, 097205 (2007).
[17] O. Boulle, V. Cros, J. Grollier, L. G. Pereira, C. Deranlot, F. Petroff, G. Faini, J. Barnaś, and A. Fert, Nat. Phys. **3**, 492 (2007).
[18] O. Boulle, V. Cros, J. Grollier, L. G. Pereira, C. Deranlot, F. Petroff, G. Faini, J. Barnaś, and A. Fert, Phys. Rev. B **77**, 174403 (2008).
[19] Y. Acremann, J. P. Strachan, V. Chembrolu, S. D. Andrews, T. Tyliszczak, J. A. Katine, M. J. Carey, B. M. Clemens, H. C. Siegmann, and J. Stöhr, Phys. Rev. Lett. **96**, 217202 (2006).
[20] D. V. Berkov and N. L. Gorn, Phys. Rev. B **72**, 094401 (2005).
[21] W. F. Brown, Phys. Rev. **130**, 1677 (1963).
[22] J. L. Garcia-Palacios and F. J. Lazaro, Phys. Rev. B **58**, 14937 (1998).
[23] P. E. Kloeden and E. Platen, *Numerical Solution of Stochastic Differential Equations* (Springer-Verlag, Berlin, 1992).
[24] S. W. Roberts, Technometrics **42**, 97 (2000).
[25] G. E. W. Bauer, Y. Tserkovnyak, D. Huertas-Hernando, and A. Brataas, Phys. Rev. B **67**, 094421 (2003).
[26] M. Gmitra and J. Barnaś, Phys. Rev. B **79**, 012403 (2009).
[27] E. E. Rodriguez, T. Proffen, A. Llobet, J. J. Rhyne, and J. F. Mitchell, Phys. Rev. B **71**, 104430 (2005).